Available online at www.sciencedirect.com
SCIENCE DIRECT®
Polymer 44 (2003) 7467–7476
polymer
www.elsevier.com/locate/polymer

# Early stages of polymer crystallization—a dielectric study

Andreas Wurm, Ragab Soliman, Christoph Schick*

*Deparment of Physics, University of Rostock, Universitätsplatz 3, 18051 Rostock, Germany*

Received 8 July 2003; received in revised form 15 September 2003; accepted 17 September 2003

**Abstract**

The existence and the formation of pre-ordered structures as the initial step during the complex process of polymer crystallization are discussed controversially. Most of the findings and interpretations are based on scattering experiments, which test small density differences between the assumed precursors of the crystals and the surrounding melt. Because of the low contrast the interpretation of experimental results become often speculative. In contrast relaxation experiments are probing motions in the sample and are therefore independent on density contrast. During crystallization, material is transformed from the liquid to the solid state. Consequently, motions typical for a liquid become impossible and do not longer contribute to the measured signal. For pre-ordered structures we expect some changes in mobility too because of the changes in conformation on pre-ordering.

We performed dielectric relaxation experiments during isothermal crystallization of PCL. Pronounced effects in $\epsilon'$ are observed long before changes in crystallinity can be detected. The observations strongly support the idea of pre-order in the polymer melt before the formation of crystals.


*Keywords:* Polymer crystallization; Early stages; Dielectric spectroscopy

## 1. Introduction

The process of polymer crystallization is a matter of debate since polymer crystals were first mentioned by Staudinger in 1927 [1]. Over the years the whole spectrum of available experimental methods was used to study the process of morphology development in polymers. Since the beginning of the 60th the Hoffmann–Lauritzen theory and several modifications and extensions of it dominate the discussion in the scientific community [2–4]. These theories assume the transition from the entangled polymer melt to the crystal, having the final thickness and stability, as a process occurring at the growth front. But there is increasing evidence that these theories do not describe the process correctly. Especially the observation of ordered structures at very early times forced the development of new theories and models [5–13]. All these theories assume a multistep process from the entangled melt via different metastable structures to the final polymer crystal. Often only the first or initiating step, as the key step for the whole process, is discussed and described. This step is assumed as spinodal decomposition [14–17] or as nucleation followed by growth [18,19]. Recently Strobl [20] introduced a model for polymer crystallization, which covers the whole process with a few specific steps. These steps are considered to be universal for polymer crystallization. The first step is assumed to be the formation of a metastable pre-ordered structure in the super cooled melt. This structure should be in thermodynamic equilibrium with the surrounding melt and should undergo different annealing stages to a stable lamella step by step. As the last step a stabilization process of the lamellae is assumed. Evidence for that comes from scattering experiments [21] and techniques probing properties like shear modulus or melting temperature rather than morphology directly [22].

In parallel to the development of new theories and models specific experiments were performed to demonstrate the existence of pre-ordered structures at the beginning of the crystallization process. Most of the experimental techniques used are scattering techniques [8,12,23–25]. But there remain a lot of open questions regarding the interpretation of the data. Interpretation is only possible if a certain structural model is assumed. Therefore up to now it was not possible to prove explicitly the existence of

* Corresponding author. Tel.: +49-381-498-6880; fax: +49-381-498-6702.
*E-mail address:* christoph.schick@physik.uni-rostock.de (C. Schick).

0032-3861/$ - see front matter © 2003 Elsevier Ltd. All rights reserved.
doi:10.1016/j.polymer.2003.09.028

pre-ordered structures. Also with AFM, which allows to follow the growth of a lamella in situ [26] it seems to be difficult to resolve the development of the first ordered structures because of low contrast.

Evidence for pre-ordered structures comes from time resolved FT-IR spectroscopy, which does not require three dimensional order. These spectra are determined by regular packing of the folded chain into the crystal lattice as well as by intramolecular conformational changes. For example, Li et al. [27] report a time shift between the appearance of the characteristic peaks for first conformational changes and of the characteristic FT-IR peaks of the crystalline phase in poly(bisphenol A-*co*-decane ether).

Nevertheless, the assumption of the formation of a mesomorphic structure as the first step in Strobl's model is yet not experimentally justified. This is mainly due to insignificant contrast for scattering and microscopic techniques commonly used to study early stages of polymer crystallization.

In contrary to these methods, where information is gained from the small contrast between the pre-ordered structure and the surrounding super cooled melt, relaxation experiments are probing motions in the sample. During crystallization material is transformed from the liquid to the solid state. Consequently, motions (fluctuations) typical for a liquid become impossible and do not longer contribute to the measured signal. Quantities like heat capacity, shear modulus or dielectric permittivity therefore allow studying crystallization. The occurrence of cooperative motions (cooperatively rearranging regions (CRR), dynamic heterogeneities) which are the reason for the liquid like heat capacity, for example, is probed by relaxation experiments [28,29]. There is no need for any density contrast to observe differences regarding mobility within the amorphous phase of a semicrystalline polymer by means of relaxation measurements. This allows a more detailed description of the semicrystalline morphology within a so called 'three phase model'. It is, for example, possible to distinguish between the mobile amorphous, the rigid amorphous and the crystalline fraction and to follow their development during crystallization [30].

Because no density contrast is needed, relaxation experiments are sensitive tools to study early stages of polymer crystallization too. Winter et al. [31] performed sheer spectroscopy experiments and showed for different polymers, that one can treat early stages of polymer crystallization like a gel formation. They discuss the formation of a network of mechanical force propagation paths as the first step of the crystallization process prior to crystal formation. Unfortunately, the relation between mechanical properties and sample morphology is very complex because of unknown details of force propagation in semicrystalline polymers [32].

For dielectric experiments the situation is different. Here the fluctuations of dipoles and charge carriers are tested only. In contrary to mechanical experiments no network for perturbation propagation is necessary. The propagation of the electrical field is easy to realize, therefore the possible frequency range for the perturbation is much broader than for other dynamic experiments. With a combination of different devices one can cover a frequency range between $10^{-6}$ and $10^{12}$ Hz and higher [29]. For the investigation of relaxation processes and conductivity dielectric spectroscopy is a frequently used method. To detect changes in morphology often the so called α-relaxation (dynamic glass transition) is followed in time or temperature [33–43].

It is assumed that, first of all, the step in the real part of dielectric permittivity is directly related to the fraction of material taking part in the relaxation process studied. The intensity of the α-relaxation (glass transition) is known to depend on the liquid fraction only. Therefore the transformation of liquid material into crystalline and rigid amorphous can be followed [44,45]. Additional information is available from the shift in relaxation time and the shape of the loss peak [45,46]. On the other hand the intensity of local relaxation processes like the β-relaxation in PET depends on the non-crystalline fraction only and allows following crystallinity directly [45]. Often not only changes in the relaxation strength but also changes in the relaxation time distribution are observed. The peak in $\epsilon''$ shifts during crystallization of homopolymers generally to lower frequencies and becomes broader [37,45,47]. Extensive studies in this field were performed by Ezquerra et al., who also combined dielectric spectroscopy with X-ray scattering for simultaneous measurements [35,36,44]. But due to the complex behavior of the α-relaxation and the crystallization process it is difficult to interpret the data.

The cooperative motions representative for the liquid behavior of the melt and detected by the α-relaxation occur on length scales of some nanometers [28,29]. As long as pre-ordering does not yield significant changes in mobility on such length scales there is basically no way to obtain information on pre-ordering from dielectric spectroscopy in the α-relaxation range. Consequently, only a few dielectric studies devoted to the early stages of polymer crystallization are available in the literature [34,41]. The information available so far does not give conclusive information about possible pre-ordering in polymers. Another unfavorable prerequisite for such type of experiments is the necessity to crystallize the sample at temperatures, where the α-relaxation can be followed in the frequency window of the dielectric device. This is usually possible at temperatures just above the thermal glass transition. For polymers one is therefore often limited to investigate cold crystallization. Cooling the sample through the maximum of the growth rate without forming crystals is not an easy task for fast crystallizing polymers. Therefore sample variety is limited. But there is another important disadvantage of cold crystallization. Also if the cooling through the maximum of crystallization rate is possible without detectable crystallization the influence of the cooling process on nucleation and the following crystallization process is well known but

not completely understood. Aging below the glass transition temperature of the amorphous polymer may influence crystallization [48], too. Consequently, for investigation of the early stages of polymer crystallization one has to take into account possible influences due to cooling and storage. Crystallizing from the glassy state generally yields smaller crystals and a larger number of spherulites, etc. Therefore it seems to be better to study crystallization at high temperatures near the melting temperature. Then the initial state of the sample, the entangled equilibrated melt, is the same for all experiments and will not significantly change at cooling from the melt to the crystallization temperature.

While at cold crystallization the dielectric response is mainly determined by the α-relaxation at higher temperatures charge carrier relaxations and conductivity may dominate the signal. Here we present dielectric studies on melt crystallization of poly (epsilon-caprolactone) (PCL). We discuss changes in the dielectric permittivity (real and imaginary part), influenced by changes in dipole and charge carrier relaxation and changes of conductivity during crystallization, especially at early times.

## 2. Experimental

The linear aliphatic polylactone poly (epsilon-caprolactone) (PCL) is a commercial sample from Aldrich with a molecular weight average of 55,700 g/mol. The dielectric properties were measured using the Broadband Dielectric Spectrometer System BDS 4000 (Alpha high resolution dielectric analyzer) from Novocontrol and a Hewlett–Packard Impedance analyzer HP 4284A. Both systems are equipped with a Quatro Cryosystem from Novocontrol for temperature control and WinDETA software version 4.1 to control the systems. The measuring cell has parallel disc geometry with an electrode diameter of 20 mm. Sample thickness was controlled by spacers of 0.15 mm thickness if not other stated and was checked using a micrometer after sample preparation. The granular, semicrystalline raw material was placed between two gold plated brass plates and heated above the melting temperature. At a pressure of 0.5 MPa, the sample was brought to its final shape.

Dielectric measurements were performed on temperature scanning and isothermally. In both cases frequency sweeps between 20 Hz and 1 MHz (HP 4284A) or 0.01 Hz and 10 MHz (Alpha analyzer) were successively repeated until the end of the experiment. The time for one frequency sweep was about 1 min for the HP 4284A and 30 min for the Alpha analyzer. For each single measuring point real and imaginary part of dielectric permittivity as well as time, temperature and frequency were recorded.

DSC scan experiments were performed at a rate of 1 K/min on cooling and heating with a PerkinElmer DSC 6. Samples of about 2 mg were placed without pan on a thin aluminum foil of about 2 mg at the sensor to reduce thermal lag as much as possible. Crystallinity as function of crystallization time was obtained from DSC scan experiments with heating rate 1 K/min utilizing a Perkin Elmer Pyris 1 DSC and a Setaram DSC 121. Sample mass was about 10 mg in the Pyris 1 DSC and 168 mg in the DSC 121. The PCL sample was heated to the melt at 70 °C after each crystallization step and the heat of fusion was determined by simple integration of the relatively sharp melting peak. Heat of fusion of the 100% crystalline PCL was assumed as 153.5 J/g [49]. The measurement was repeated for other times and other temperatures as needed. PCL is thermally very stable. No changes after several crystallization-melting cycles were detected.

## 3. Results

We first checked the influence of crystallization and melting on the dielectric permittivity at cooling and heating. In Fig. 1, real and imaginary part of the dielectric permittivity at 20 Hz and 10 kHz as well as the specific heat flow from a DSC experiment for PCL are shown for cooling at 1 K $min^{-1}$, followed by heating at 1 K $min^{-1}$.

Real and imaginary part of the dielectric permittivity coincides in the melt for each frequency on cooling and on heating between 60 and 70 °C. Therefore the identical state can be assumed before crystallization and after melting. The experiment was repeated several times to check reproducibility and stability of the sample. Two scan experiment with

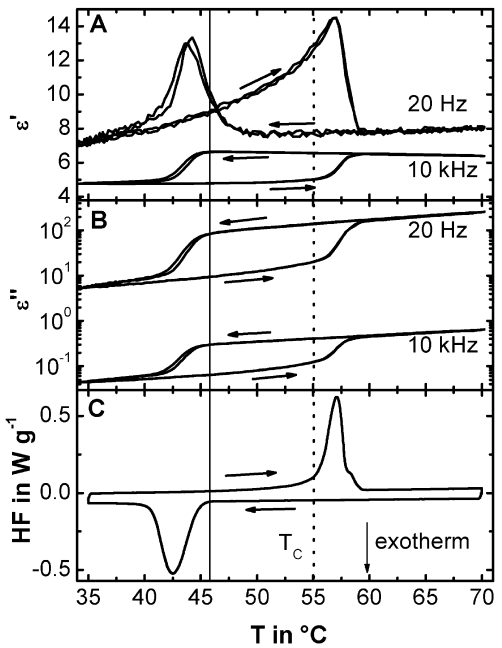


Fig. 1. Real part $\epsilon'$ (A) and imaginary part $\epsilon''$ (B) of dielectric permittivity $\epsilon^*(\omega) = \epsilon' - i\omega\epsilon''$ at cooling of PCL followed by heating at rate 1 K $min^{-1}$ (two independent measurements) at 20 Hz and 10 kHz. Specific heat flow HF (C) from a DSC experiment at the same scanning rates. The vertical dotted line at 55 °C indicates the crystallization temperature for the isothermal crystallization experiments shown below. Sample thickness 0.15 mm.

the same time–temperature profile are shown in Fig. 1A and B. The two independent experiments coincide and yield the same crystallization kinetics. This was also checked for all following isothermal experiments. No differences in the behavior of permittivity were observed for equal experimental conditions.

At crystallization a decrease and at melting an increase of dielectric permittivity is expected because of the changing number of mobile dipoles and charge carriers contributing to the signal. The imaginary part $\epsilon''$ (part B) shows the expected dependencies at crystallization and melting for all frequencies studied (only two are shown). The real part $\epsilon'$ (part A) at high frequencies (10 kHz) also behaves as expected. But the curves at 20 Hz are unexpected. At crystallization and at melting a peak in $\epsilon'$ is observed. Interestingly, at cooling the peak onset appears at approximately 4 K higher temperature compared to the first changes detected in the heat flow rate (part C) or in $\epsilon''$ (part B), see vertical line at 46 °C.

The differences in the absolute values of permittivity in Fig. 1 result from the frequency dependence of charge carrier relaxations. As lower the frequency as higher is their contribution to permittivity. The increase in $\epsilon'$ at low frequencies is commonly interpreted as an interfacial relaxation process (Maxwell Wagner Sillars or electrode polarization). The peak seen in $\epsilon'$ at 20 Hz at crystallization and melting may be related to such processes because of the formation and disappearance of interfaces during the course of crystallization and melting, respectively.

Similar results were found during crystallization and melting of PET. But for PET the maximum is not as pronounced as for PCL. Additionally α-relaxation and melting and re-crystallization processes affect dielectric permittivity in the interesting frequency range. Therefore we have performed more detailed experiments with PCL only.

One possibility for an increasing real part of permittivity is the occurrence of the α-relaxation or local relaxation processes in the frequency-temperature window of the experiment. To know the position of the relaxation processes dielectric spectra of semicrystalline PCL were analyzed in a wider temperature range.

The frequencies of the loss peak maxima for the different relaxation processes in semicrystalline PCL as a function of reciprocal temperature are shown in Fig. 2. The points were obtained from isothermal frequency sweeps between −150 and 0 °C for every 10 K. The dielectric permittivity was measured in the frequency range $10^{-2}$ to $10^{6}$ Hz. To illustrate the complex relaxation behavior permittivity curves for five representative temperatures are shown in Fig. 3.

At temperatures above 0 °C charge carrier relaxations became dominant in the $\epsilon'$ curves at low frequencies. Therefore these effects cannot be neglected for further discussion of the maximum observed at crystallization and melting for PCL. At the crystallization temperature

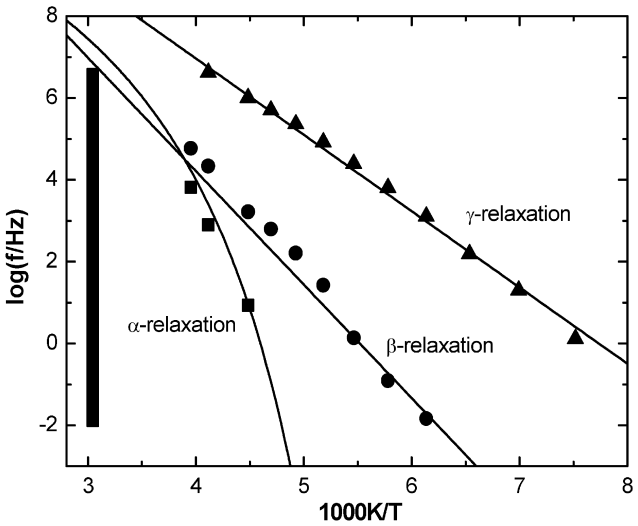


Fig. 2. Activation diagram for PCL from isothermal dielectric experiments; lines from [50]; symbols this work. The points represent the frequency of the dielectric loss maximum for the fit functions according to Havriliak and Negami [51], see Fig. 3. The vertical bar indicates the frequency–temperature range for further isothermal crystallization experiments.

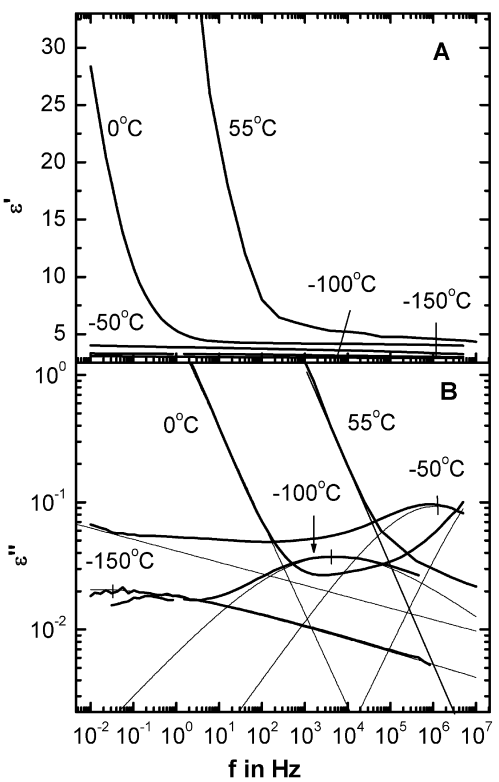


Fig. 3. Frequency dependence of the real part $\epsilon'$ (A) and imaginary part $\epsilon''$ (B) of dielectric permittivity of PCL at different temperatures (−150, −100, −50, 0 and 55 °C). The thin lines in B represent fit-curves taking into account one or two Havriliak–Negami functions and a conductivity term [51] at −50, 0 and 55 °C. The short vertical bars indicate the position of the maximum of the fit curves which are shown in the Arrhenius-diagram (Fig. 2).

(between 40 and 55 °C) the maximum positions of all other relaxation processes are above 1 MHz. Therefore for PCL the observed maximum at 20 Hz is not due to one of the relaxation processes shown in Fig. 2. To obtain more detailed information about the whole crystallization process and possible reasons for the observed maximum in $\epsilon'$ we performed isothermal crystallization experiments.

To be able to resolve all stages during the complex crystallization process one has to choose temperatures with slow crystallization kinetics. This is usually the case near the melting temperature. For isothermal crystallization of PCL the crystallization process is reasonable slow above 50 °C. We used a temperature of 55 °C for our detailed studies. This temperature is indicated as the dashed line in Fig. 1. At this temperature the experiments in the frequency range between $10^{-2}$ Hz and 1 MHz are not influenced by the α-relaxation. But as shown in Fig. 3, curve at 55 °C, charge carrier relaxations and conductivity dominate permittivity of the thin semicrystalline PCL sample at frequencies below $10^3$ and $10^5$ Hz for the real and the imaginary part, respectively. The frequency dependency of permittivity of the super cooled melt and its development during isothermal crystallization can be seen from Fig. 4. The sample was cooled from the melt at 70 °C to the crystallization temperature at 1 K $min^{-1}$. Frequency sweeps were successively repeated every 2100 s. At 55 °C and before crystallization sets in $\epsilon'$ is frequency independent at frequencies above 40 Hz. During the isothermal experiment the frequency dependence does not change until 10,000 s. But the curve observed at 20,000 s is significantly different compared to the earlier curves. At the lowest frequencies this is the result of decreasing electrode polarization, whereas in the frequency range between 10 and $10^3$ Hz a new process which is introduced during main crystallization is observed. For a more detailed discussion of the time dependences of $\epsilon'$ and $\epsilon''$ the data presented in Fig. 4 are shown in Fig. 5 as a function of time for the different frequencies.

A continuous decrease of $\epsilon'$ and $\epsilon''$ with time is observed at low and high frequencies. But at intermediate frequencies between 2.5 and 250 Hz a maximum in $\epsilon'$ occurs again. The very large values of $\epsilon'$ at low frequencies, Figs. 4 and 5, are due to charge carrier relaxations. Because the high values appear from the very beginning of the isothermal experiment, when the sample is in the isotropic liquid state, electrode polarization rather than Maxwell Wagner Sillars relaxation seems to be the reason for the observed large values. To reduce the contribution from electrode polarization one can measure samples with a reduced electrode surface to volume ratio. That's why we have measured a sample with 20 mm diameter and 5 mm thickness. The results for an isothermal crystallization experiment at 52 °C are shown in Figs. 6 and 7.

First of all the values of $\epsilon'$ at low frequencies are drastically reduced. This proves that electrode polarization is the reason for the high values seen in Figs. 4 and 5 for the thinner sample. On the other hand, the maximum in $\epsilon'$ is

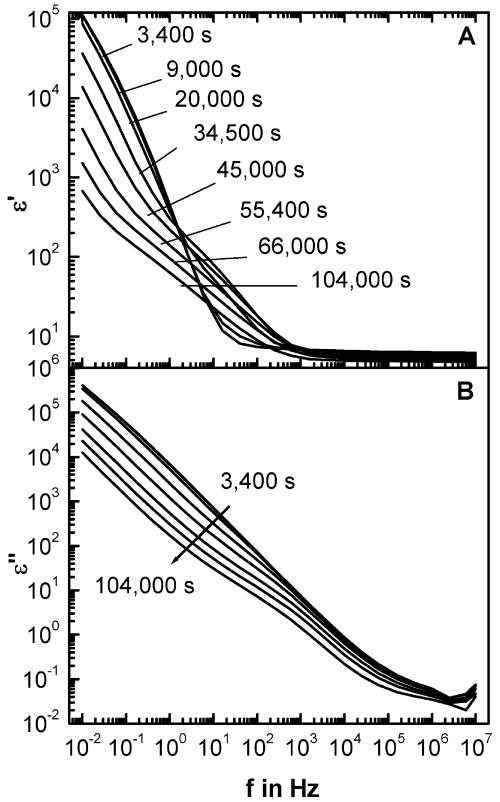


Fig. 4. Frequency dependence of the real part $\epsilon'$ (A) and imaginary part $\epsilon''$ (B) of permittivity during isothermal crystallization of PCL at 55 °C at different times. Sample thickness 0.15 mm.

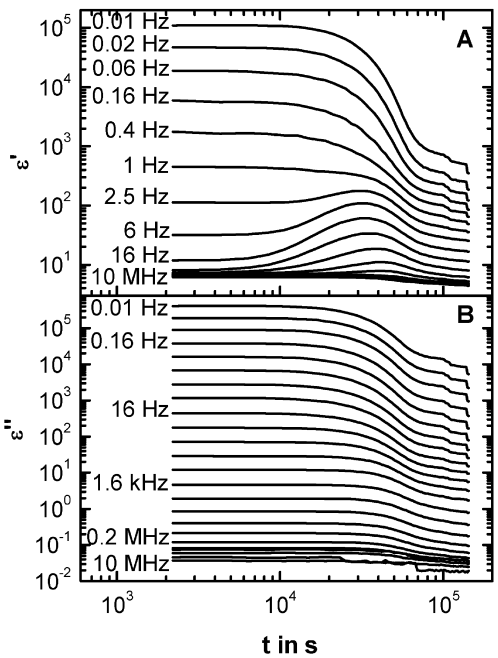


Fig. 5. Time dependence of the real part $\epsilon'$ (A) and imaginary part $\epsilon''$ (B) of permittivity during isothermal crystallization of PCL at 55 °C at different frequencies between $10^{-2}$ and $10^7$ Hz. Real part as well as imaginary part decreases at all times with increasing frequency. Sample thickness 0.15 mm.

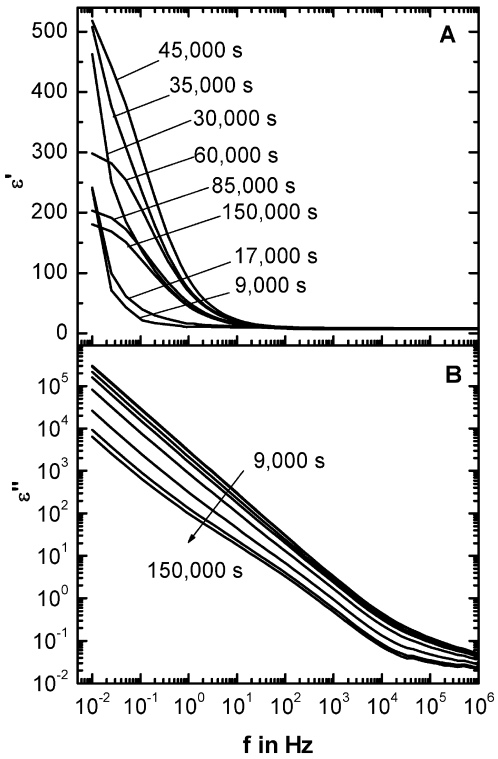


Fig. 6. Frequency dependence of the real part $\epsilon'$ (A) and imaginary part $\epsilon''$ (B) of permittivity during isothermal crystallization of PCL at 52 °C at different times. Sample thickness 5 mm.

now seen in all curves for frequencies below 10 Hz. Even at the lowest frequency of 0.01 Hz the maximum is well pronounced. But the increase of $\epsilon'$ starts despite the lower crystallization temperature after longer annealing times

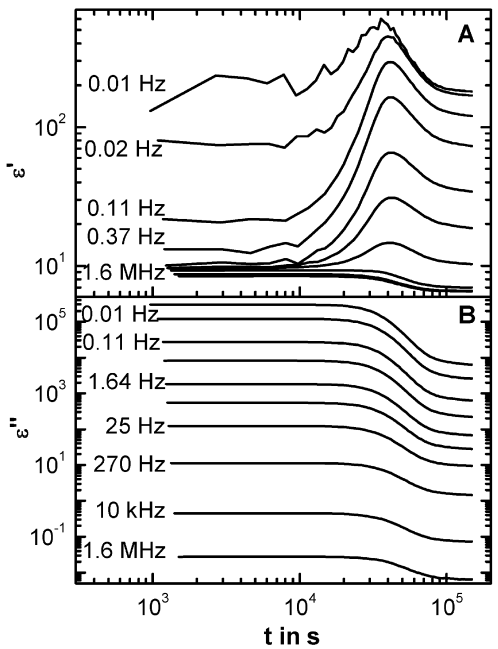


Fig. 7. Time dependence of the real part $\epsilon'$ (A) and imaginary part $\epsilon''$ (B) of permittivity during isothermal crystallization of PCL at 52 °C at different frequencies between 0.01 and $1.6 \times 10^6$ Hz. Sample thickness 5 mm.

compared to the thin samples. Interestingly, there is, as for the thin sample, no frequency dependence of the peak location in time. The whole crystallization process shows a slower kinetic instead of the expected faster kinetic because of the lower temperature. Crystallization kinetics seems to depend on sample thickness. This effect is often observed when crystallization begins at the surfaces of the sample and proceeds later in the bulk. For thicker samples, the surface to volume ratio becomes smaller and therefore crystallization kinetics becomes slower. A similar effect was observed for the crystallization kinetics in the DSC. The thin sample measured in the Perkin Elmer DSC 6 crystallized much faster than a ca. 5 mm diameter cylindrically sample measured in the Setaram DSC 121. Nevertheless, the occurrence of the maximum at low frequencies for the thick sample and the comparable maximum values of $\epsilon'$ in the medium frequency range show that electrode polarization or some changes in the polymer morphology close to the surface at the early stages of crystallization (trans crystallinity [52]) cannot be the reason for the observed maximum in $\epsilon'$.

To allow a more quantitative discussion of the curves shown in Figs. 5 and 7 we compare the time dependencies of permittivity with the time dependence of the non-crystalline fraction during the course of isothermal crystallization, see Figs. 8 and 9. From DSC scans of comparable thick samples to the melt (70 °C) after annealing at the crystallization temperature we obtained crystallinity from $\chi_c = \Delta H/\Delta H^0$ where $\Delta H$ equals the measured heat of fusion and $\Delta H^0$ equals the heat of fusion of the infinite large crystal at the melting temperature ($\Delta H^0 = 153.5\ \mathrm{J\ g^{-1}}$). The non-crystalline fraction was obtained from $\chi_{nc} = 1 - \chi_c$. For seek of clarity permittivity and non-crystalline fractions are scaled such way that in the melt (short times) and in the semicrystalline sample (at the end of the measurement) both curves coincide.

The decrease in the non-crystalline fraction starts after the induction period of crystallization at about 20,000 s, see points in Figs. 8 and 9. At high frequencies, the curve at $10^6$ Hz is shown as an example, $\epsilon'$ and $\epsilon''$ follow the non-crystalline fraction during the whole course of crystallization. Such behavior is expected from the decreasing number of mobile dipoles and limited charge carrier mobility with increasing crystallinity. This result shows that in both devices, dielectric spectrometer and calorimeter, crystallization kinetics is the same. Beside the unexpected maximum at intermediate frequencies the curves at low frequencies deviate significantly from the decrease of the non-crystalline fraction, $10^{-2}$ Hz is shown as an example in Fig. 8 and $2.5 \times 10^{-2}$ Hz in Fig. 9. Especially $\epsilon'$ starts to decrease for the thin sample much earlier than the non-crystalline fraction. At such low frequencies $\epsilon'$ is mainly determined by electrode polarization for the thin sample. The early decrease of $\epsilon'$ shows that charge carrier mobility is reduced due to some structure formation different from crystal formation (main crystallization).

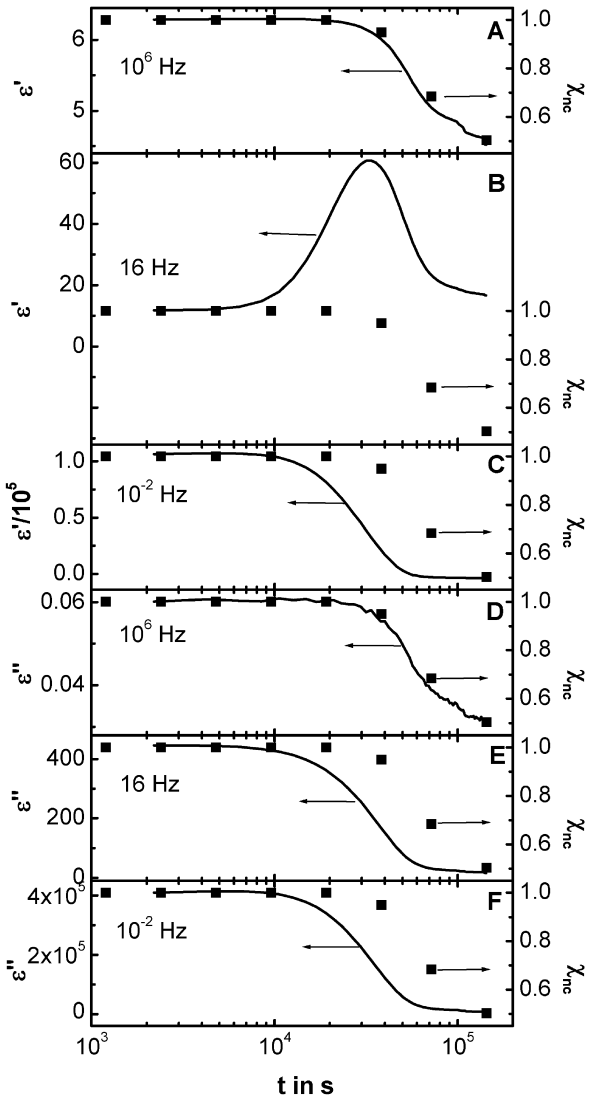


Fig. 8. Time dependence of the real part $\epsilon'$ (A–C) and imaginary part $\epsilon''$ (D–F) of permittivity during isothermal crystallization of PCL at 55 °C at frequency $10^6$ Hz (A and D), 16 Hz (B and E) and $10^{-2}$ Hz (C and F). The squares represent the amount of amorphous material after different times of isothermal crystallization obtained from DSC experiments. Sample thickness 0.15 mm.

Next, we compare permittivity with the non-crystalline fraction at frequencies between 2.5 and 250 Hz (thin sample) and below 100 Hz (thick sample) where the maximum in $\epsilon'$ occurs, see Figs. 5 and 7. The maximum in $\epsilon'$ is observed between 30,000 and 40,000 s (thin sample) and at about 40,000 s (thick sample). The increase in $\epsilon'$ starts already at about 6000 s. This is again long before the non-crystalline fraction from DSC starts to decrease. The value of the dielectric constant after crystallization is for these frequencies higher than the value in the melt before crystallization. For $\epsilon''$, see Figs. 8E and 9D the behavior is qualitatively the same as for the low frequency shown in Fig. 8F.

To check possible temperature dependencies of the observed peak in $\epsilon'$ the measurements were repeated for the

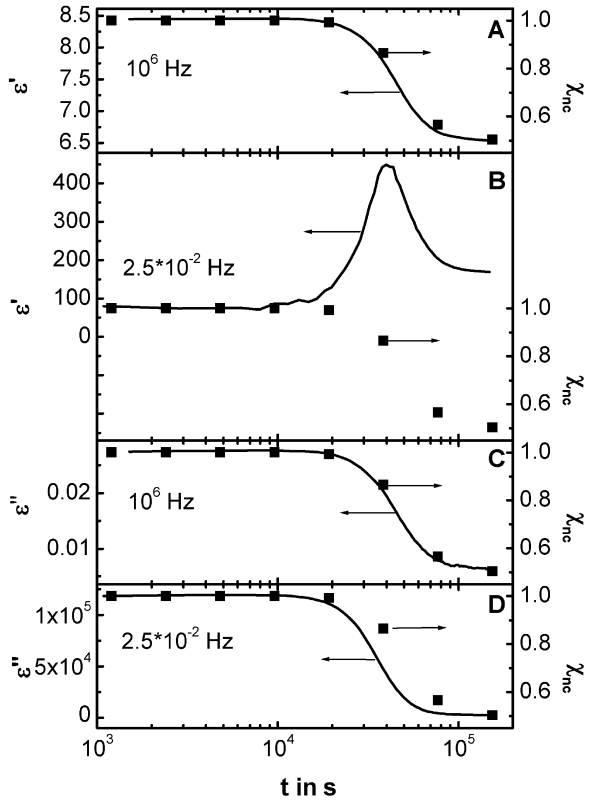


Fig. 9. Time dependence of the real part $\epsilon'$ (A and B) and imaginary part $\epsilon''$ (C and D) of permittivity during isothermal crystallization of PCL at 52 °C at frequency $10^6$ Hz (A and C) and $2.5 \times 10^{-2}$ Hz (B and D). The squares represent the amount of amorphous material after different times of isothermal crystallization obtained from DSC experiments. Sample thickness ca. 5 mm.

thin sample at different temperatures. To be able to follow faster crystallization the frequency range was limited, 20 Hz to 900 kHz. Frequency sweeps were repeated successively for every 30 s utilizing the HP 4284A. In Fig. 10

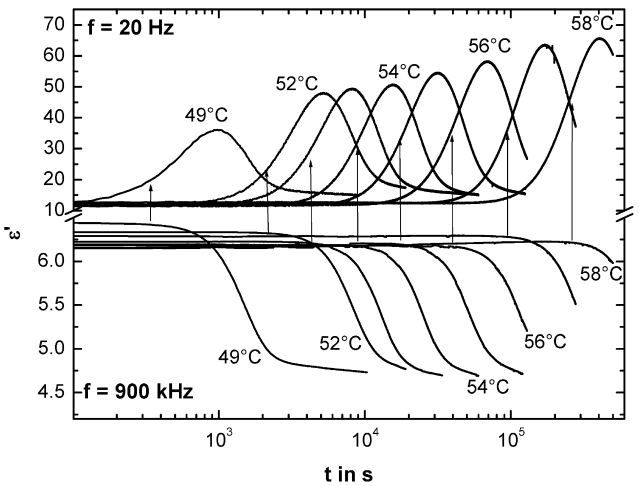


Fig. 10. Time dependencies of the real part $\epsilon'$ of the dielectric function during isothermal crystallization of PCL at different temperatures at frequency 20 and 900 kHz. The arrows indicate the beginning of the decrease of $\epsilon'$ at 900 kHz for the different temperatures. Sample thickness 0.15 mm.

permittivity during isothermal crystallization at different temperatures between 49 and 58 °C at frequency 20 Hz and 900 kHz is shown for the thin sample. The shift of the crystallization process to shorter times at lower temperatures results from the increase of the crystallization rate with decreasing temperature. Whereas $\epsilon'$ measured at 900 kHz behaves always proportional to the decrease of the non-crystalline fraction, $\epsilon'$ measured at 20 Hz shows always a peak. The arrows in Fig. 10 indicate the starting point of the decrease of $\epsilon'$ at 900 kHz. This is the beginning of crystal formation at the specific crystallization temperature. The increase at 20 Hz starts always significantly earlier. The maximum values of $\epsilon'$ increase with increasing crystallization temperature.

The occurrence of such pronounced maxima over time requires at least two competing processes. The decrease of $\epsilon'$ at longer times during main crystallization is due to decreasing mobility of relaxing dipoles and charge carriers. The reason for the increase at shorter times is not as clear. In Section 4, we will discuss this in more detail.

## 4. Discussion

We would like to answer the question: how can we understand the maximum in $\epsilon'$ and the early decrease of permittivity at low frequencies for the thin sample during isothermal crystallization? We divide the discussion in three parts: (i) the high frequency range, were dipole relaxations can be followed without contributions from charge carrier relaxation and conductivity, (ii) contributions from electrode polarization for the thin sample at low frequencies, and (iii) the unexpected maximum in $\epsilon'$ at frequencies where electrode polarization can be neglected.

(i) The measurements during isothermal crystallization of PCL were performed at such high temperatures that the dispersion zones of dipole relaxation process, like α-relaxation (dynamic glass transition) or β- and γ-relaxation (local relaxations) are above the frequency window of the measurements discussed here, see Fig. 2. Therefore all dipoles are relaxed and contribute to permittivity. At frequencies higher than $10^3$ Hz for $\epsilon'$ and $10^5$ Hz for $\epsilon''$ contributions from charge carriers to permittivity can be neglected. During crystallization at least the dipoles, which are incorporated into the crystalline regions will no longer contribute to permittivity because of the missing mobility. With ongoing crystallization, consequently, a decrease of $\epsilon'$ as well as of $\epsilon''$ is expected and seen in Figs. 8A, D and 9A, C. The comparison with the decreasing non-crystalline fraction during crystallization shows a perfect agreement. This expected behavior at high frequencies is also a proof for identical crystallization kinetics in the dielectric measuring cells and the calorimeters. Main parameter for identical kinetics is an identical sample temperature. Therefore we can be sure to have same crystallization temperatures in the different devices. Also the influence of sample thickness on crystallization kinetics is well reproduced in dielectric and DSC measurements.

(ii) For the thin sample electrode polarization yield the extremely high values of permittivity at low frequencies. This was proved by measurements with a much thicker sample, which does not show such large values. Electrode polarization is due to charge carriers traveling between the electrodes and yielding an electric double layer at the electrodes. These double layers increases real and imaginary part of permittivity. For DC conductivity, in contrast, only a contribution to $\epsilon''$ is expected. For the isothermal crystallization experiments we observe a monotone decrease of permittivity, see Fig. 8C and F. The interesting point here is the very early decrease of permittivity compared with the decrease of the non-crystalline fraction in the sample. There must be a decrease of the number of charge carriers traveling between the electrodes. For the main crystallization one can expect a decreasing number of mobile charge carriers because some of them will be incorporated in the crystals and will be blocked. But at the very early stages it is hard to imagine that charge carriers are blocked by the assumed pre-ordered structures or some nuclei. It seems to be more reasonable to assume a reduction of mobility of the charge carriers. May be this reduction of mobility is due to some trapping of charge carriers at the interfaces of the pre-ordered structures. Because the decrease in $\epsilon'$ and $\epsilon''$ starts significantly earlier than the decrease of the non-crystalline fraction other structures than crystals formed in the bulk must be considered to explain the observed behavior. Electrode polarization is related to charge carriers traveling between the electrodes. To affect mobility on such length scales it needs structures influencing the whole sample volume and not only small spots like nuclei.

(iii) The contribution of electrode polarization to permittivity can be reduced by much thicker samples or higher frequencies. As can be seen in Fig. 6, were electrode polarization is prevented by using larger sample thickness we see some peculiarity starting at the same time as the reduction of electrode polarization discussed in (ii). Also for the thin sample at medium frequencies we observe a maximum in $\epsilon'$ and a decrease in $\epsilon''$ starting at the same times as the decrease of electrode polarization. Because electrode polarization can be neglected under these particular conditions electrode polarization and processes related to the interaction between electrode and sample cannot be the origin of the increasing $\epsilon'$ seen in Figs. 5 and 7.

The observed maximum in $\epsilon'$ can also not be explained by changing dipole mobility during crystallization because this always results in a decrease of $\epsilon'$, as discussed in section (i). Electrode polarization alone cannot explain the observed maximum because it appears also under experimental conditions where electrode polarization is avoided due to larger sample thickness, as shown in Fig. 7, or higher frequencies, see Fig. 5 at frequencies between 2.5 and

250 Hz. The reason for the increase and the resulting maximum in $\epsilon'$ between 30,000 and 40,000 s in the frequency range under consideration must be another one. The increase of $\epsilon'$ can only be explained under the assumption of at least one additional process. This process, which is not present in the super-cooled, equilibrated melt, appears during annealing at the crystallization temperature. The increasing permittivity can only be explained by an additional dipole moment, as e.g. discussed for a cross linking system [53], or by the formation of additional internal surfaces, which results in a Maxwell Wagner Sillars process different from electrode polarization. These additional dipole moments or interfaces must be created before crystallinity can be detected by DSC. The result is an increasing permittivity during the induction period of isothermal crystallization. The formation of really crystalline structures on the other hand reduces dipole and charge carrier mobility and consequently the permittivity decreases with ongoing time yielding in the superposition the maximum in $\epsilon'$. The point of inflection in the rising flank of the peak appears just at the moment when crystal formation starts and some dipole and charge carrier relaxations are freezing. The corresponding times for the different temperatures are marked in Fig. 10 by arrows. With increasing crystallinity more and more dipole and charge carrier relaxations are hindered and $\epsilon'$ finally decreases. This is in analogy to the behavior at high frequencies, see Figs. 8 and 9.

The formation of new molecular dipoles before crystallization seems unrealistic. Therefore the formation of internal surfaces and the resulting Maxwell Wagner Sillars process seems responsible for the increasing $\epsilon'$. This must happen long before crystal formation. But how one can understand the appearance of additional surfaces in the melt before crystal formation? One possibility would be the known surface induced crystallization at the electrodes. The result would be a thin crystalline layer, which covers the electrodes. The dielectric contrast between the remaining amorphous sample and the crystalline layers would result in an additional Maxwell Wagner Sillars process (electrode polarization) and consequently an increasing permittivity. For electrode polarization the mean relaxation time $\tau_{EP}$ is given as [29]

$$\tau_{EP} \approx \frac{\epsilon_S \epsilon_0}{\sigma_0} \frac{D}{2l_D} \quad (1)$$

where $\epsilon_0$ is vacuum permittivity, $\epsilon_S$ is static permittivity, $\sigma_0$ is d.c.-conductivity, $D$ is sample thickness and $l_D$, the effective thickness of the double layer at the electrodes. If a transcrystalline layer influences $l_D$ one would expect a shift towards higher frequency with increasing transcrystalline layer thickness. This is not observed in our measurements. The position of the peak in $\epsilon'$ is frequency independent.

With increasing sample thickness one would expect a shift towards lower frequencies and the influence of electrode polarization would become smaller. This is observed in Fig. 6 compared to Fig. 4. But the measurement in Fig. 7 shows also for a 5 mm thick sample a peak in $\epsilon'$, which is comparable to the thin sample. Therefore the formation of thin crystalline layers directly at the electrodes cannot be the origin of the additional internal surfaces with dielectric contrast. It has to be a bulk property.

In Fig. 5 in the frequency range between 16 and 100 Hz, $\epsilon'$ stays constant at the end of the crystallization process, but at a higher value compared to the super cooled melt. The same is observed for the thicker sample at frequencies below 100 Hz, see Fig. 7. In the just described picture, this is only possible if the newly formed surfaces survive main crystallization together with the corresponding Maxwell Wagner Sillars process, what seems to be reasonable.

Let us assume pre-ordered structures in a polymer melt before crystal formation as discussed by Strobl [20]. During pre-ordering a quasi parallel alignment of chain segments lead to the formation of a mesomorphic phase with additional internal surfaces between the mesomorphic structures and the surrounding entangled polymer melt. Our results can be explained by such a picture.

## 5. Conclusion

During the crystallization of PCL pronounced effects in $\epsilon'$ are observed before changes in crystallinity can be detected. Especially for isothermal crystallization two observations strongly support the idea of pre-order in the polymer melt before the formation of crystals. (i) Electrode polarization is reduced significantly before crystallinity changes can be detected. Indicating that the structure formation at early stages reduces charge carrier mobility on length scales comparable with sample thickness. (ii) In cases where electrode polarization is not dominating permittivity an increase in $\epsilon'$ due to the formation of internal surfaces and finally a maximum is observed. The increase in $\epsilon'$ starts again much earlier than changes in crystallinity can be detected. The start time of the increase in $\epsilon'$ corresponds to the start time of the reduction of electrode polarization.

The structures formed at the early stages of polymer crystallization reduce charge carrier mobility on the length scale related to electrode polarization (comparable to sample thickness). The same structures yield additional Maxwell Wagner Sillars relaxation processes, which result in an increase of $\epsilon'$. The reduction of the large scale charge carrier movements (reduction of electrode polarization) supports the idea of large scale structures formed at the early stages of polymer crystallization rather than the formation of a large number of small structures (nuclei).

## Acknowledgements

This work was financially supported by the German

Science Foundation (DFG) Grant Schi 9-1 and the Government of Egypt. We acknowledge valuable discussions with A. Schönhals, Berlin, I. Alig, Darmstadt, and F. Kremer, Leipzig.

## References

[1] Staudinger H, Johner H, Signer R, Mie G, Hengstenberg J. Mitt Chem Phys Inst Freiburg 1927;425–88.
[2] Lauritzen JI, Hoffmann JD. Nat Bur Stand 1959;31:1680–1.
[3] Sadler DM. Polymer 1983;24:1401–9.
[4] Gedde UW. Polymer physics. London: Chapman and Hall; 1995. pp. 169–98.
[5] Acierno S, Grizzuti N, Winter HH. Macromolecules 2002;35:5043–8.
[6] Samon JM, Schultz JM, Hsiao BS. Polymer 2002;43:1873–5.
[7] Kumaraswamy G, Verma RK, Issaian AM, Wang P, Kornfield JA, Yeh F, Hsiao BS, Olley RH. Polymer 2000;42:8931–40.
[8] Wang ZG, Hsiao BS, Sirota EB, Srinivas S. Polymer 2000;41: 8825–32.
[9] Pogodina NV, Siddiquee SK, van Egmond JW, Winter HH. Macromolecules 1999;32:1167–74.
[10] Pogodina NV, Winter HH. Macromolecules 1998;31:8164–72.
[11] Wang ZG, Hsiao BS, Sirota EB, Agarwal P, Srinivas S. Macromolecules 2000;33:978–89.
[12] Albrecht T, Strobl G. Macromolecules 1996;29:783–5.
[13] Paternostre L, Damman P, Dosiere M. Polymer 1998;39:4579–92.
[14] Olmsted PD, Poon WCK, Mcleish TCB, Terrill NJ, Ryan AJ. Phys Rev Lett 1998;81:373–6.
[15] Imai M, Kaji K, Kanaya T, Sakai Y. Phys Rev B 1995;52:12696–704.
[16] Imai M, Mori K, Mizukami T, Kaji K, Kanaya T. Polymer 1992;33: 4451–6.
[17] Doi M, Shimada T, Okana K. J Chem Phys 1988;88:4070–5.
[18] Muthukumar M, Welch P. Polymer 2000;41:8833–7.
[19] Meyer H, Müller F-P. Macromolecules 2002;35:1241–52.
[20] Strobl G. Eur Phys J E 2000;3:165–83.
[21] Heck B, Hugel T, Iijima M, Sadiku E, Strobl G. Polymer 2000;41: 8839–48.
[22] Wurm A, Schick C. e-Polymer 2002;art. no. 0 24:1–15.
[23] Schultz JM, Hsiao BS, Samon JM. Polymer 2000;41:8887–95.
[24] Ryan AJ, Fairclough JPA, Terrill NJ, Olmsted PD, Poon WCK. Faraday Discuss 1999;112:13–30.
[25] Matsuba G, Kaji K, Kanaya T, Nishida K. Phys Rev E 2002;65: 61801–7.
[26] Hobbs JK, Humphris ADL, Miles MJ. Macromolecules 2001;34: 5508–19.
[27] Jiang Y, Gu Q, Li L, Shen DY, Jin XG, Chan CM. Polymer 2003;44: 3509–13.
[28] Donth E, Glass transition, Berlin: Springer; 2001.
[29] Kremer F, Schönhals A, Broadband dielectric spectroscopy, Heidelberg: Springer; 2002.
[30] Schick C, Wurm A, Mohammed A. In: Sommer JU, Reiter G, editors. Polymer crystallization: observations, concepts and interpretations. Berlin: Springer; 2002. p. 253–80.
[31] Schwittay C, Mours M, Winter HH. Faraday Discuss 1995;101: 93–104.
[32] Perez J. Polym Sci B 1998;40:17–46.
[33] Nogales A, Ezquerra TA, Denchev Z, Balta-Calleja FJ. Polymer 2001; 42:5711–5.
[34] Ezquerra TA, Lopezcabarcos E, Hsiao BS, Baltacalleja FJ. Phys Rev E 1996;54:989–92.
[35] Ezquerra TA, Baltacalleja FJ, Zachmann HG. Polymer 1994;35: 2600–6.
[36] Ezquerra AT, Majszczyk J, Baltacalleja JF, Lopezcabarcos E, Gardner HK, Hsiao BS. Phys Rev B 1994;50:6023–31.
[37] Dobbertin J, Hannemann J, Schick C, Pötter M, Dehne H. J Chem Phys 1998;108:9062–8.
[38] Mijovic J, Sy JW. Macromolecules 2002;35:6370–6.
[39] Tombari E, Ferrari C, Salvetti G, Johari GP. J Phys: Condens Matter 1999;11:A317–27.
[40] Andjelic S, Fitz BD. J Polym Sci B 2000;38:2436–48.
[41] Fukao K, Miyamoto Y. Phys Rev Lett 1997;79:4613–6.
[42] Massalskaarodz M, Williams G, Smith IK, Conolly C, Aldridge GA, Dabrowski R. J Chem Soc -Faraday Transact 1998;94:387–94.
[43] Saad GR, Mansour AA, Hamed AH. Polymer 1997;38:4091–6.
[44] Sics I, Ezquerra TA, Nogales A, Denchev Z, Alvarez C, Funari SS. Polymer 2003;44:1045–9.
[45] Schick C, Dobbertin J, Pötter M, Dehne H, Hensel A, Wurm A, Ghoneim AM, Weyer S. J Therm Anal 1997;49:499–511.
[46] Hardy L, Stevenson I, Boiteux G, Seytre G, Schönhals A. Polymer 2001;42:5679–87.
[47] Boyd RH, Liu F. In: Runt JP, Fitzgerald JJ, editors. Dielectric spectroscopy of polymeric materials. Washington: ACS; 1997. p. 107–36.
[48] Okamoto N, Oguni M, Sagawa Y. J Phys-Condens Matter 1997;9: 9187–98.
[49] Wunderlich B. et al. See on www url: http://web.utk.edu/(athas/databank/intro.html.
[50] Grimau M, Lardo E, Perez MC, Bello A. J Chem Phys 2001;114: 6417–25.
[51] Havriliak S, Negami S. J Polym Sci C 1966;14:99–117.
[52] Liu J, Li H, Yan S, Xiao Q, Petermann. J Coll Polym Sci 2003;281: 601–7.
[53] Salehli F, Kamer O, Catalgil-Giz H, Giz A, Yildiz G. J Non-Cryst Solids 2002;305:183–9.